

Supporting Information

Acid- and Base-Resistant Antimicrobial Hydrogels based on Polyoxometalates and Chitosan

Callum McWilliams,^{a,b} Isabel Franco-Castillo,^{a,b} Andrés Seral Ascaso,^{a,b} Sonia García-Embid,^{a,b} Mariella Malefioudaki,^{a,b} Johann G. Meier,^c Rafael Martín-Rapún*,^{a,b} Scott G. Mitchell*^{a,b}

a Instituto de Nanociencia y Materiales de Aragón (INMA), CSIC-Universidad de Zaragoza, c/Pedro Cerbuna 12, 50009 Zaragoza, Spain.

b CIBER de Bioingeniería, Biomateriales y Nanomedicina, Instituto de Salud Carlos III, 28029 Madrid, Spain.

c ITAINNOVA – Instituto Tecnológico de Aragón, Calle María de Luna, n° 7, Zaragoza, 50018, Spain.

* corresponding author email: scott.mitchell@csic.es

Keywords: Polyoxometalate, chitosan, hydrogels, antimicrobial materials, acid-resistance, base-resistance

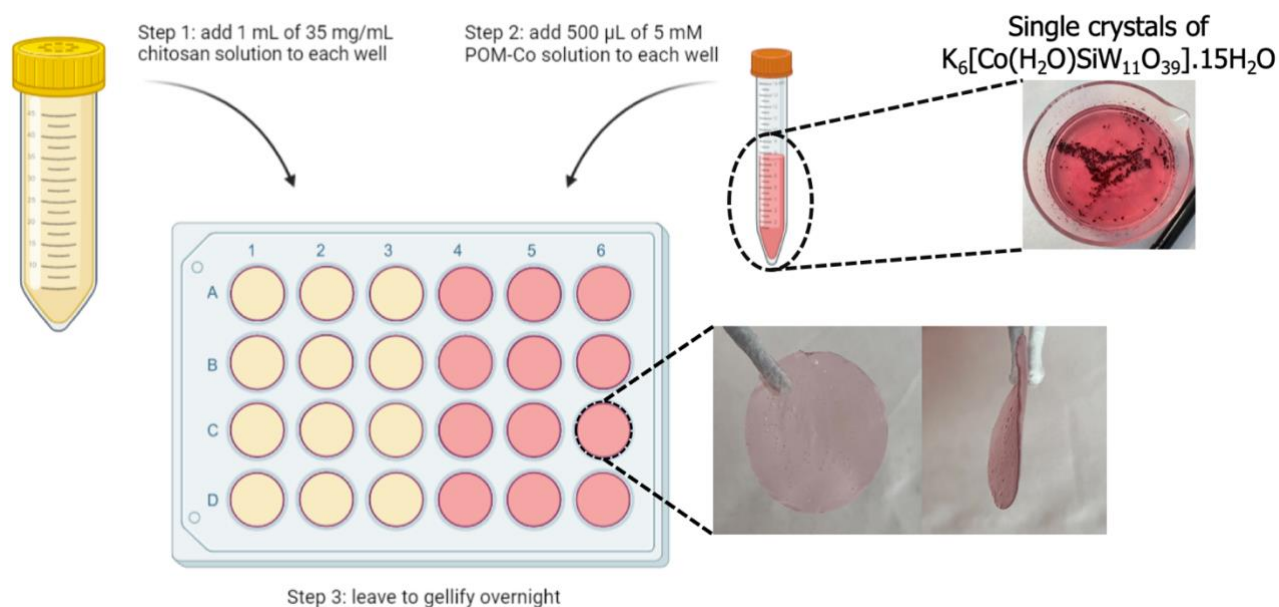


Figure S1. Schematic illustration of the synthesis of the $CoSiW_{11}@CS$ hydrogel.

Supporting Information

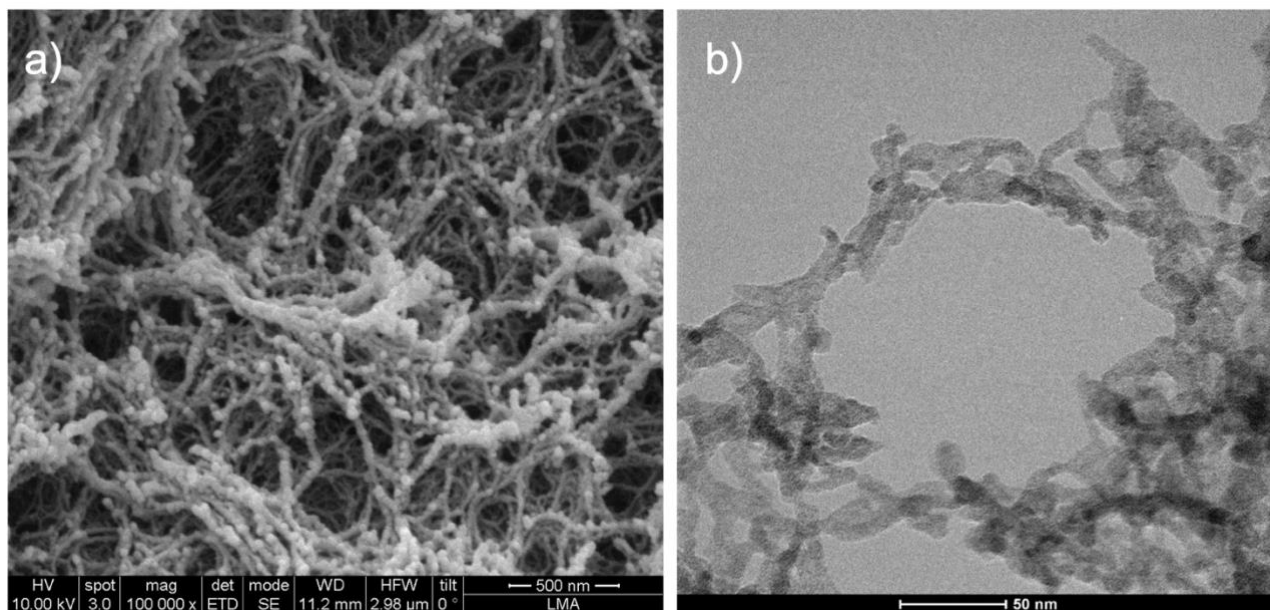


Figure S2. a) SEM and b) TEM images of CoSiW₁₁@CS after supercritical drying and coating with Au/Pd.

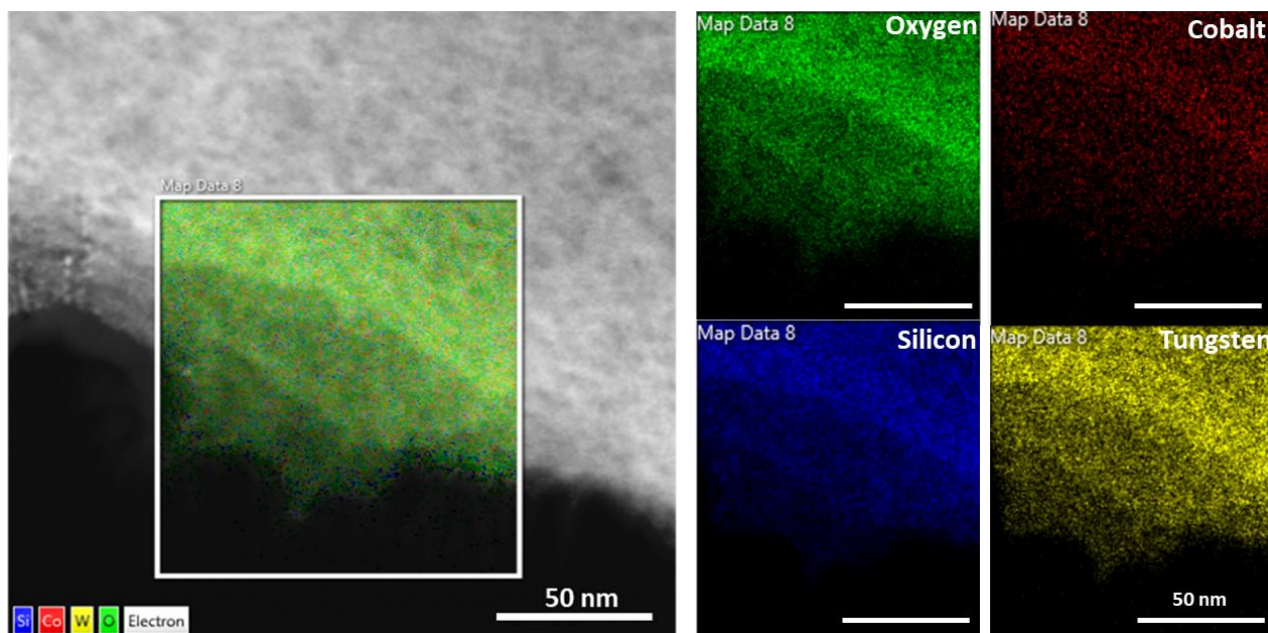


Figure S3. EDS imaging, via TEM, displaying the homogeneous dispersion of the elements of K₆[Co(H₂O)SiW₁₁O₃₉] throughout the CoSiW₁₁@CS hydrogel.

Supporting Information

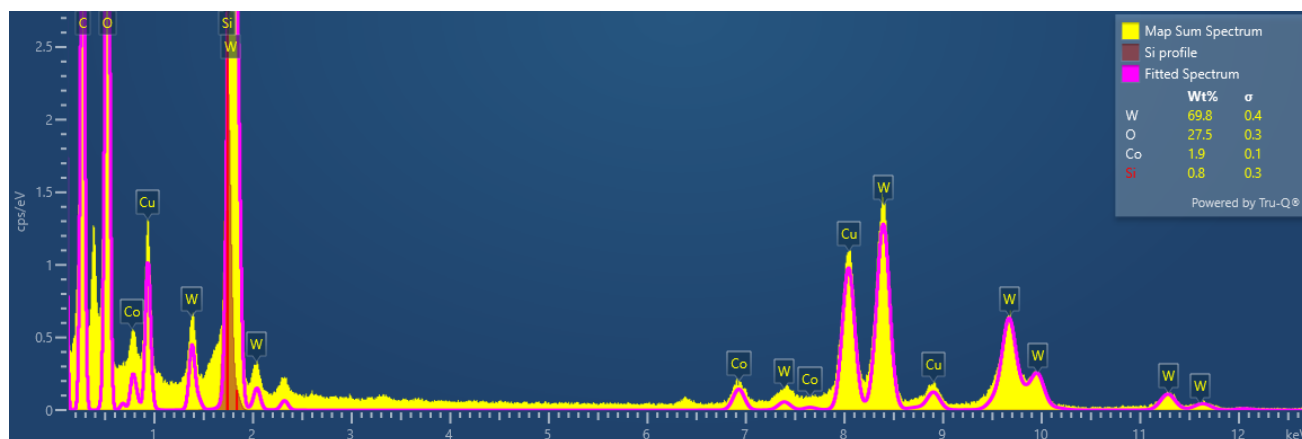


Figure S4. Corresponding EDS spectrum of CoSiW₁₁@CS. Note that the presence of Cu and C peaks corresponded to the copper TEM grid coated in carbon.

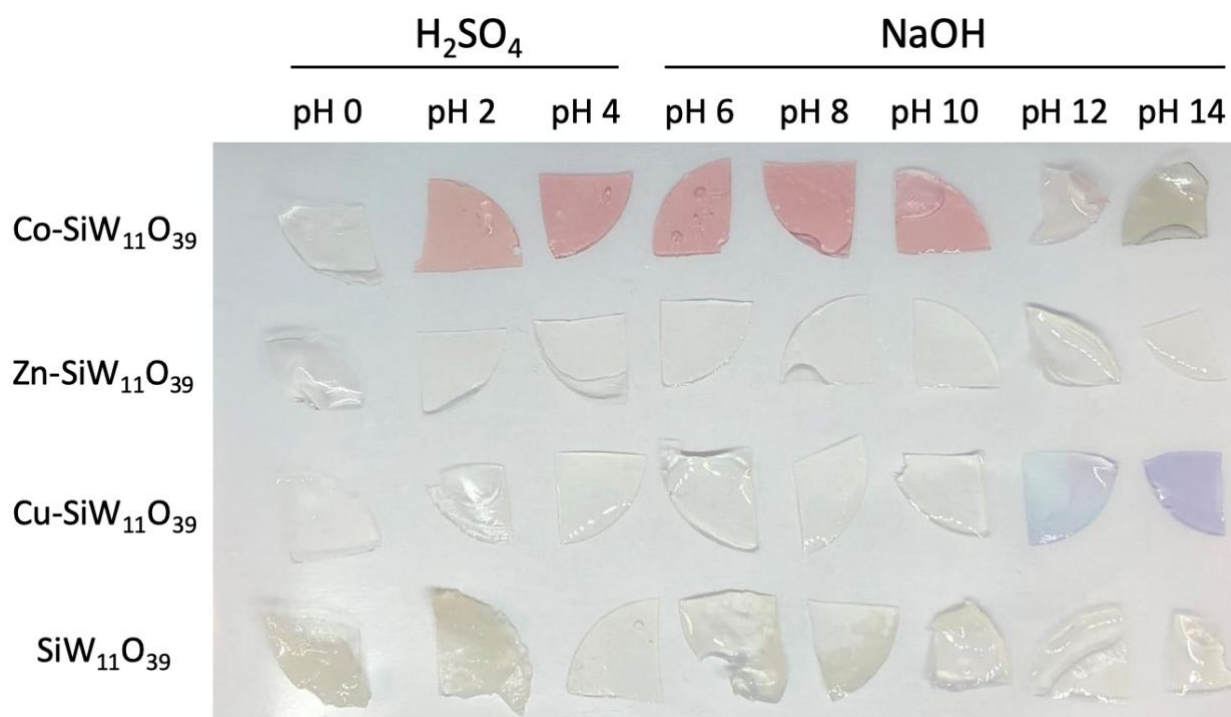


Figure S5. POM@CS hydrogels after 24 hours in solutions of different pH.

Supporting Information

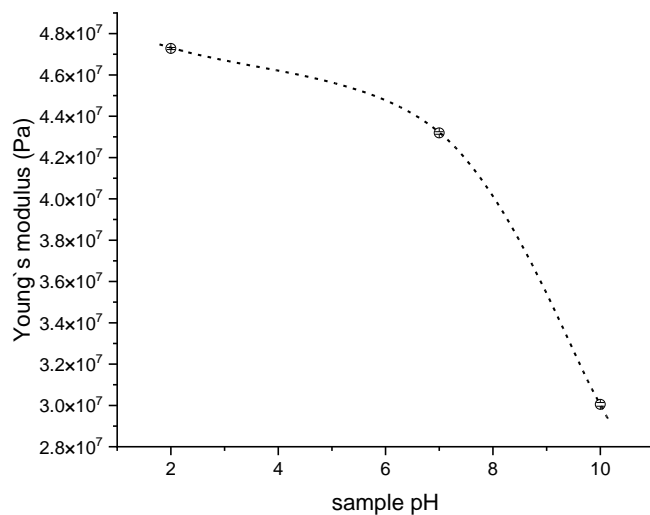
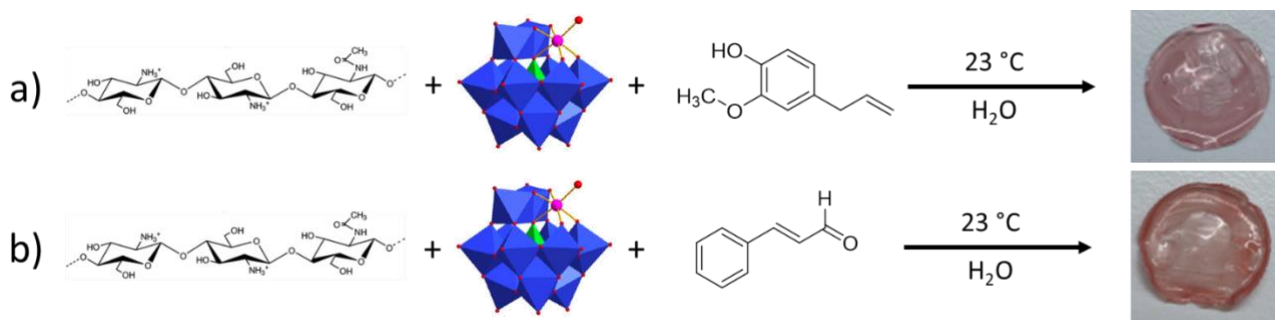


Figure S6. Young's modulus as a function of pH. The dotted line represents a guide for the general tendency of poorer stability and toughness at higher pH values.



Eugenol

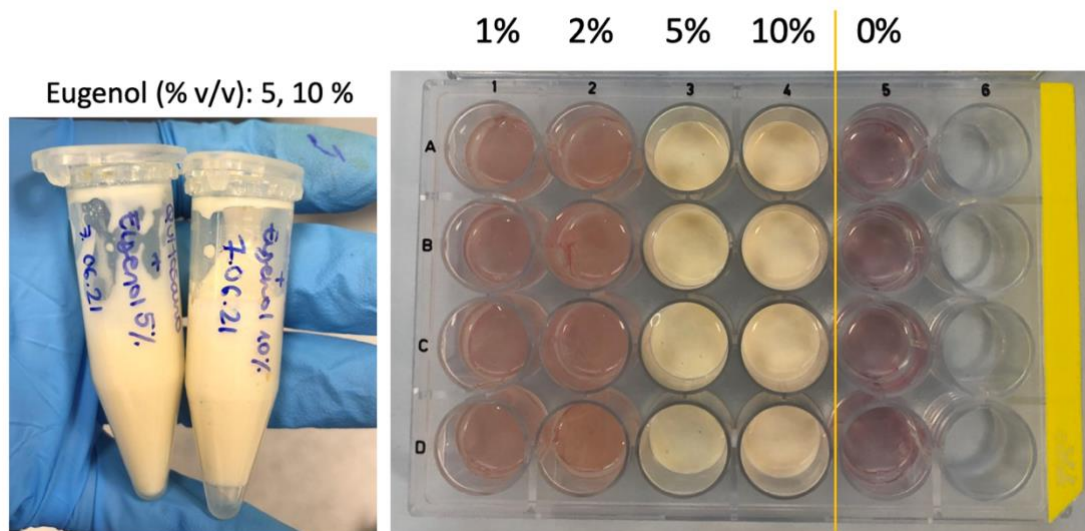


Figure S7. Synthesis of the CoSiW₁₁@CS@oil hydrogels with: a) eugenol, b) cinnamon oil. Below: chitosan solution and the corresponding essential oil were added to an Eppendorf vial and emulsified using a sonic tip and placed in well-plates for gelation.

Supporting Information

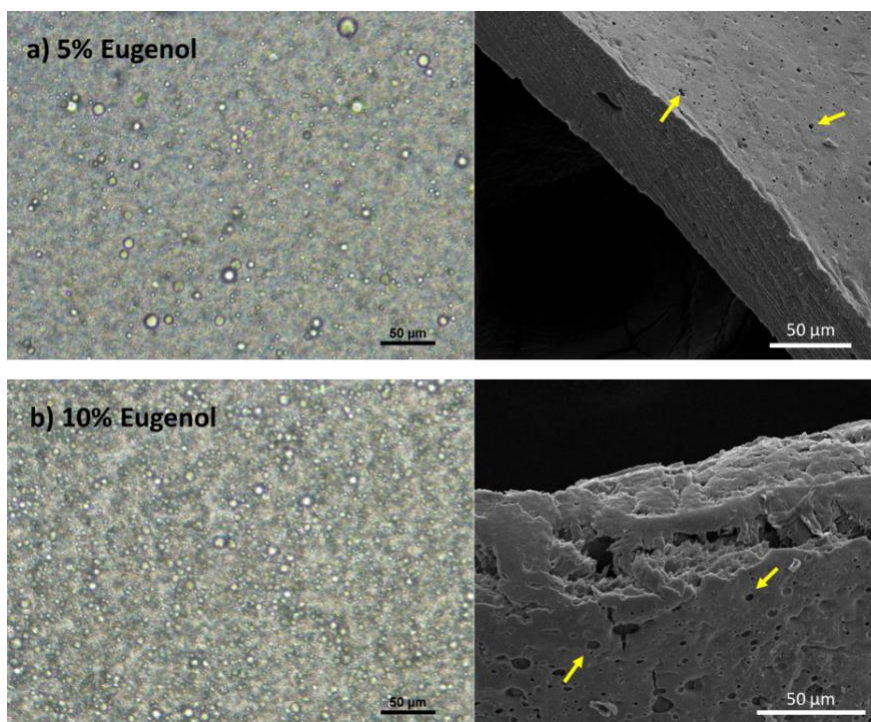


Figure S8. Optical microscopy imaging of 5 and 10% CoSiW₁₁@CS@oil hydrogels (doped with eugenol) with yellow arrows on the SEM images highlighting the oil droplets in the hydrogel.

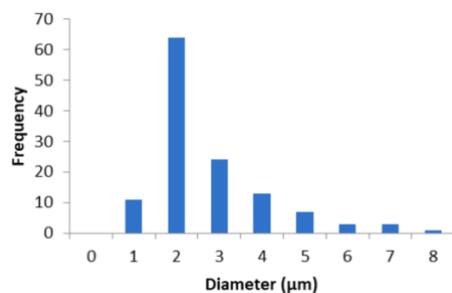


Figure S9. Size dispersion histogram of the oil droplets contained in CoSiW₁₁@CS@oil hydrogels. Data obtained from ImageJ measurements of the oil droplet diameters obtained from SEM images.

Table S1. Minimum Inhibitory Concentration (MIC) values: starting materials, eugenol, and cinnamaldehyde.

Compound	MIC (mg/mL)	
	<i>E. coli</i>	<i>B. subtilis</i>
K ₈ [α-SiW ₁₁ O ₃₉]	>12.68	12.68
Chitosan	0.25	0.15
Eugenol	0.50	0.50
Cinnamaldehyde	0.625	0.625

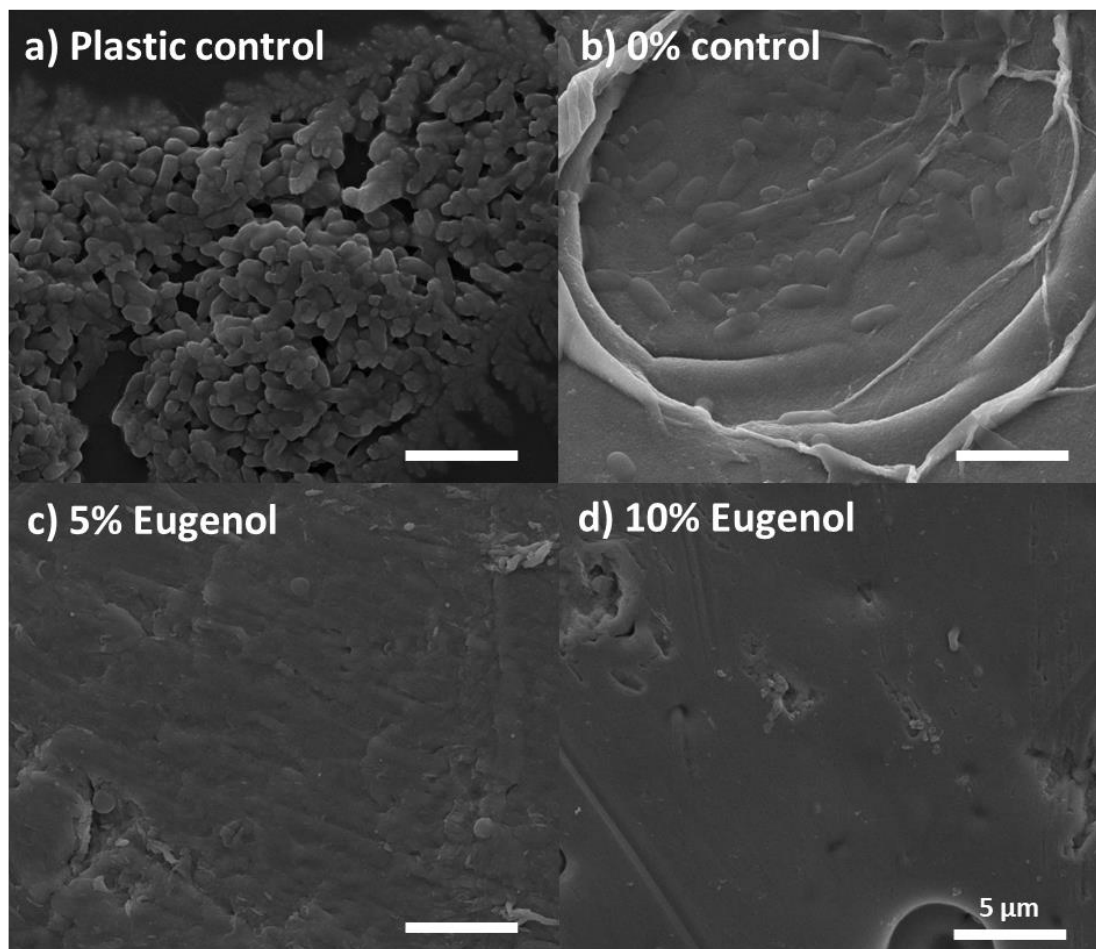


Figure S10. SEM imaging of washed samples; a) plastic control sample, b) CoSiW₁₁@CS hydrogel (0% oil content) and eugenol doped CoSiW₁₁@CS hydrogels; c) 5%, and d) 10%, after antibiofilm assay with *B. subtilis*.

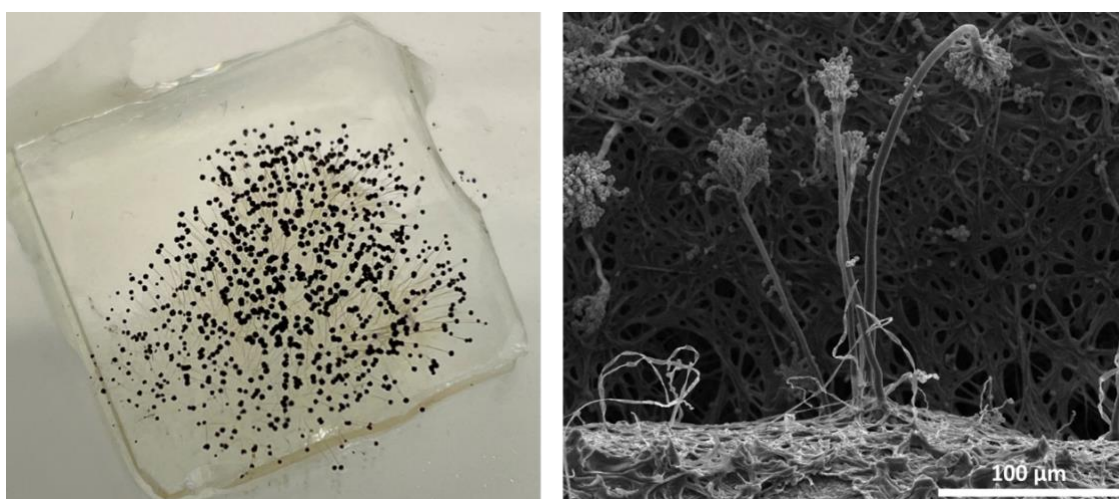


Figure S11. Conidiophores and conidia of *A. niger* visualised on the glass control sample (from the antifungal assay) and SEM imaging.

Supporting Information

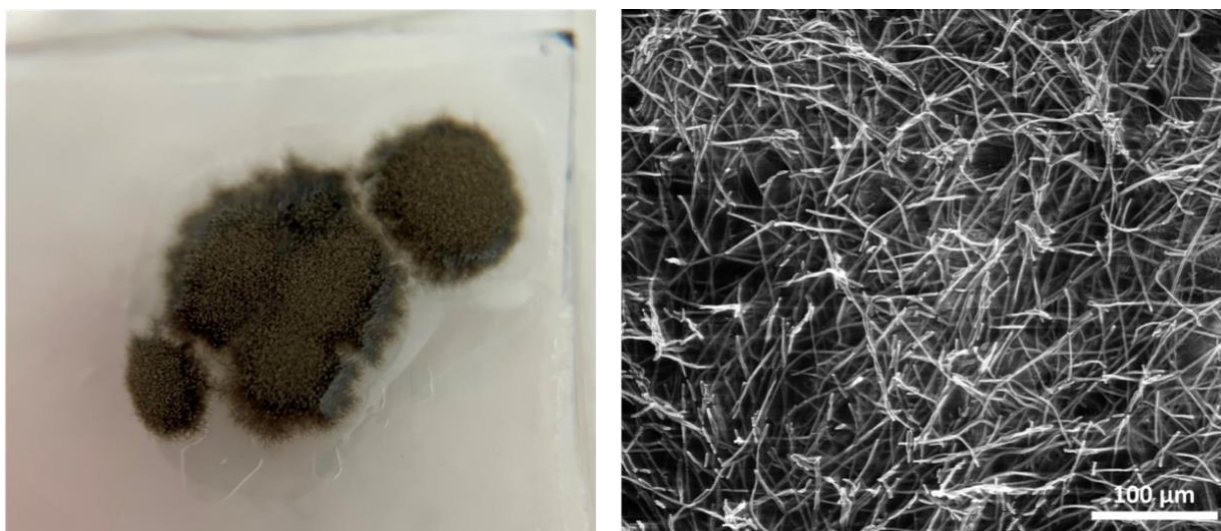


Figure S12. *C. cladosporioides* mould visualised on the glass control sample (from the antifungal assay) and SEM imaging.

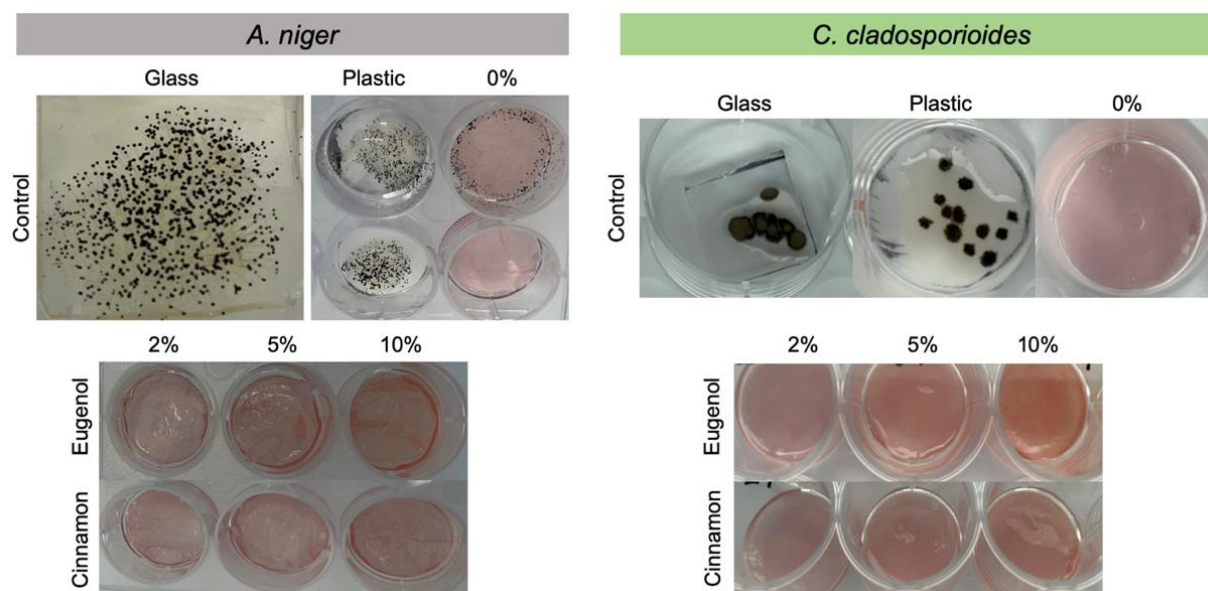


Figure S13. Performance of the CoSiW₁₁@CS and CoSiW₁₁@CS@oil hydrogels in antifungal assays against *A. niger* and *C. cladosporioides*, demonstrating the absence of fungal growth on CoSiW₁₁@CS and CoSiW₁₁@CS@oil hydrogels, compared with control growth on glass and on plastic.